# Electrochemical Evaluation of Binding Affinity for Aptamer Selection Using the Microarray Chip

*Ye Zhu*,[a] *Pranjal Chandra*,[a] *Changill Ban*,[b] *Yoon-Bo Shim**[a]

[a] Department of Chemistry and Institute of BioPhysico Sensor Technology, Pusan National University, Busan 609-735, South Korea
[b] Department of Chemistry, Pohang University of Science and Technology, San31, Hyoja-dong, Pohang, Gyungbuk, 790-784, South Korea
*e-mail: ybshim@pusan.ac.kr

Received: December 29, 2011
Accepted: February 20, 2012

**Abstract**
Simultaneous evaluation of the binding affinity of a series of aptamers toward a target molecule was investigated using an electrochemical microarray chip. The chip was modified by immobilizing seven aptamers obtained from the SELEX process and a control sequence onto gold nanoparticle-comprised conducting polymer-coated microarray electrodes. The chip was then incubated with the target molecule, kanamycin. The electrochemical response of the captured kanamycin was studied to evaluate the binding affinity of the aptamers, which showed the same trend with the fluorescence spectroscopic results. The lowest dissociation constant between a selected aptamer and kanamycin was determined to be $38.06 \pm 0.73$ nM.

**Keywords:** Aptamer, Binding affinity, Electrochemical method, Dissociation constant, Microarray chip

DOI: 10.1002/elan.201100734

## 1 Introduction

Aptamers are oligonucleotides that are capable of specifically recognizing and binding a wide range of targets with high affinity, such as small molecules, nucleic acids, proteins, cells, tissues, and organisms [1,2]. Due to the unique advantages of their in vitro synthesis, chemical component, high purity, ease of modification, and high stability, aptamers have emerged as a strong competitor of antibodies for the analysis of small molecules, for which antibodies are difficult to develop [3]. In contrast to the in vivo development of antibodies, aptamers are derived from a large random sequence pool through iterative rounds of in vitro selection and amplification using a process called Systematic Evolution of Ligands by Exponential Enrichment (SELEX) [4,5]. A series of aptamers obtained through the cloning step during the SELEX process retains similar consensus sequences that enable these aptamers to recognize and bind to their specific target. The degree of the complexation between each aptamer and the target, however, is different due to the discrepant parts of these aptamer sequences and their secondary structures [6–8]. Therefore, identifying the individual aptamer that possesses the highest affinity to the target from the series of aptamers is a critical step during the aptamer selection procedure and has recently attracted wide interest. The technique that is conventionally used for this purpose involves the determination of the dissociation constant ($K_d$) of the aptamer-target complex using fluorescence spectroscopy [9–11]. Recently, surface plasmon resonance [12–14], capillary electrophoresis [15,16], and some other methods [17] have also been reported. These methods, however, are expensive, complicated, time-consuming, and most significantly, require additional labeling processes. Thus, it is valuable to develop a direct, simple, fast, and low-cost method for the evaluation of aptamer binding affinity.

Electrochemical methods, which are generally simple and inexpensive, have been widely applied to detect molecules by using aptamers [18], however, they have not been adequately explored for the selection of high-affinity aptamers from a series of aptamers that are obtained from the cloning step during the SELEX process. The redox peaks that are exhibited in voltammograms show the electrochemical property of the tested species and also reflect their complex formation with the ligands [19]. That is, the specific peak position recorded for an electroactive molecule that is involved in complexation shifts relative to that of the free form without complexation. Moreover, the extent of the peak potential shift depends on the degree of complexation [20]. This phenomenon provides insight into the binding behavior of the target molecule with each respective ligand. Thus, it is possible to use electrochemical method to explore this complexation reaction principle and evaluate the binding affinity of aptamer toward small molecules (e.g., antibiotics and endocrine disruptors), most of which are electroactive. To our knowledge, the use of electrochemical method in exploring the binding of a series of aptamers (obtained from the cloning in SELEX) to their specific target and

  

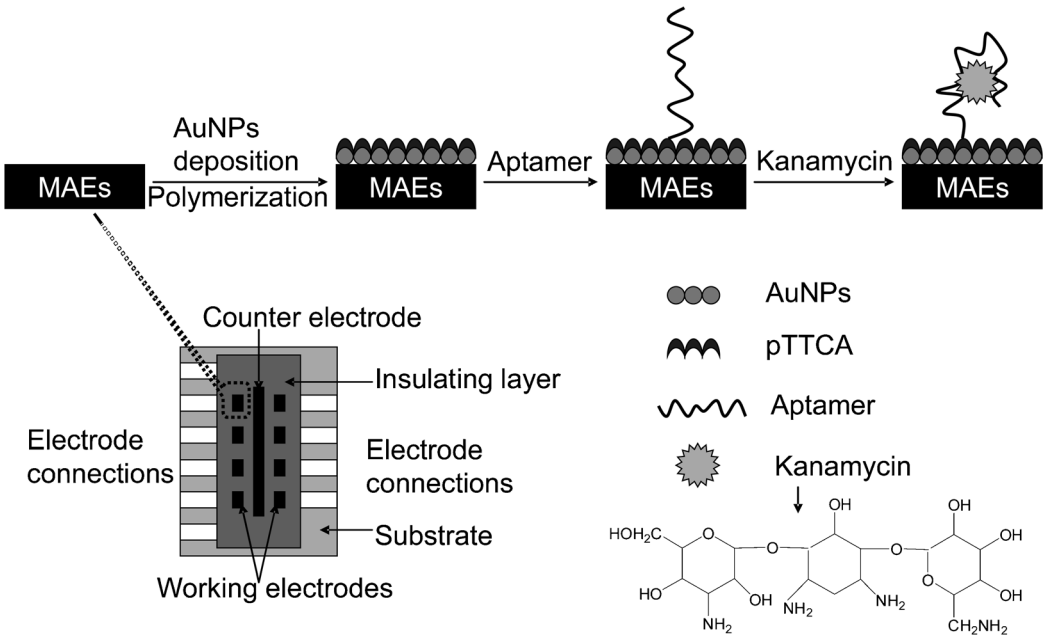


Fig. 1. Schematic representation of the MAEs chip and the modification representation for the working electrodes.

evaluating the binding affinity of these aptamers have not yet been reported. Furthermore, this will provide a new approach for the screening of aptamers for small molecules.

To demonstrate this approach, an aminoglycoside antibiotic, kanamycin (the structure is shown in Figure 1), was used as a model compound. Seven aptamers for it with similar conserved sequences were selected through the SELEX process. Subsequently, the binding affinity of the selected aptamers toward the target molecule, kanamycin, was simultaneously evaluated using microarray electrodes (MAEs) on a chip, which was modified by covalently immobilizing the seven aptamers and a random control ssDNA sequence onto gold nanoparticle (AuNP)-comprised conducting polymer-coated MAEs. The direct electrochemistry of the captured kanamycin was investigated in terms of potential shifts and current responses using cyclic voltammetry (CV) and linear sweep voltammetry (LSV) to evaluate the binding affinity of the aptamers. The $K_d$ value between each aptamer and kanamycin was determined based on the current responses and was compared with fluorescence spectroscopic results. The aptamer secondary structures that were predicted by a web-based *m*-fold program [21] were analyzed based on the electrochemical data.

## 2 Experimental

### 2.1 Chemicals and Materials

Seven amine-terminated DNA aptamers for kanamycin were selected from the cloning step in SELEX as reported earlier [22] and were obtained from Bioneer Corporation (South Korea) in addition to a random amine-terminated control ssDNA sequence that was designed by us. TE buffer, which was prepared with 10 mM tris(hydroxymethyl)aminomethane and 1 mM ethylenediaminetetraacetic acid and was adjusted to pH 8.0 with HCl, was used to dilute the aptamers and the control sequence. Kanamycin sulfate was obtained from Generay Biotech Co., Ltd. A terthiophene monomer bearing carboxylic acid group, 5,2′:5′,2″-terthiophene-3′-carboxylic acid (TTCA), was synthesized as reported earlier [23]. Gold(III) chloride trihydrate ($HAuCl_4$), 1-ethyl-3-(3-dimethylaminopropyl) carbodiimide (EDC), *N*-hydroxysuccinimide ester (NHS), di(propylene glycol) methyl ether, and tri(propylene glycol) methyl ether were purchased from Sigma-Aldrich (USA). All other chemicals were of extra-pure analytical grade and were used without further purification. All aqueous solutions were prepared in doubly distilled water that was obtained from a Milli-Q water purification system (18 MΩ cm).

### 2.2 Apparatus

The screen-printed MAEs chip, which consisted of eight working electrodes (400 μm × 400 μm each) and a counter electrode, was prepared using a model BS-450HT screen-printing machine from BANDO industrial (South Korea). An external Ag/AgCl (in saturated KCl) electrode was used as the reference electrode. To accurately compare the potential shifts of the kanamycin redox peak, the Ag/AgCl reference electrode was adjusted in $K_3[Fe(CN)_6]$/$K_4[Fe(CN)_6]$ solution before each measurement. CVs and LSVs were performed with a multichannel potentiostat/galvanostat, Kosentech (South Korea) and an EG & G PAR model 273A (USA). XPS experiments were performed using a VG scientific ESCA lab 250 XPS spec-

  

trometer coupled with a monochromated Al Kα source with charge compensation, at the Korea Basic Science Institute (Busan, South Korea). A freely available web-based *m*-fold software was used to construct the secondary structures of the aptamers.

### 2.3 Fabrication of the MAEs Chip

The MAEs chip was fabricated using a screen-printing machine (model BS-450HT). A pictorial representation of the fabricated chip is shown in Figure 1. First, silver ink was printed onto a polyethylene sheet, which was allowed to dry for 10 min to form a conductive layer. Then, the carbon ink was partially printed onto the silver layer and was dried at 60 °C for 10 min. Finally, a nonconducting insulation layer was printed to cover the nonworking surface, leaving 8 (4×2) carbon-working electrodes in array and a counter electrode in the center. An external Ag/AgCl (saturated KCl) reference electrode was used in combination with the chip.

### 2.4 Modification of the MAEs Chip and Measurements

The modification of the MAEs chip was performed with the procedure that is presented in Figure 1. First, AuNPs were electrodeposited onto the working electrodes of the chip by potential scanning three times from 1.4 V to 0.5 V in a 0.5 M $H_2SO_4$ solution containing 0.001 % $HAuCl_4$ [24,25]. During the electrodeposition of the AuNPs, the gold reduction peak was observed at 0.95 V. The peak current increased with the increasing potential sweeps, indicating the formation and growth of the AuNPs on the MAE surfaces. Thereafter, pTTCA film was allowed to form on the AuNP-deposited MAE surfaces as reported earlier [25,26]. In brief, 3 μL of a 1 mM TTCA monomer solution that was prepared in a 1:1 mixture of di(propylene glycol) methyl ether and tri(propylene glycol) methyl ether was dropped onto the AuNP-deposited MAEs. After drying, CV was performed for the polymerization of TTCA by cycling the potential twice from 0.0 to 1.5 V (vs. Ag/AgCl) at 0.1 V/s in 10 mM PBS (pH 7.4). During the anodic scan, an oxidation peak of TTCA monomer was observed at around 1.02 V. The oxidation peak current increased with the increasing potential cycle number, indicating the formation and growth of the polymer film on the MAE surfaces. The pTTCA/AuNP-coated MAEs chip was immersed in a 10 mM EDC/NHS solution to activate the carboxylic acid groups of pTTCA. Thereafter, the amine-terminated aptamers and control ssDNA sequence were immobilized by dropping 5 μL of a 10 μM solution containing one of the aptamers or control sequence onto the activated pTTCA/AuNPs/MAE surfaces and incubating at room temperature overnight, followed by washing with TE buffer to remove the unimmobilized sequences. In order to investigate the binding between the immobilized sequences and kanamycin, the aptamer- and control ssDNA-immobilized pTTCA/AuNPs/MAEs were incubated in 0.1 M PBS (pH 7.2) containing kanamycin for 20 min at 55 °C. After washing, CVs and LSVs were performed between −0.1 V and 0.5 V (vs. Ag/AgCl) at a scan rate of 0.02 V/s in 0.1 M PBS (pH 7.2) to study the electrochemical behavior of the kanamycin that was captured by the aptamers on the MAEs.

### 2.5 Comparative Analysis of Binding Affinity Using Fluorescent Measurement

Kanamycin and M-280 Tosylactivated magnetic beads were mixed and incubated with shaking for 20 h at room temperature in a coupling buffer (0.1 M borate, 0.67 M $(NH_4)_2SO_4$, pH 9.5). Then, the kanamycin-immobilized magnetic beads were incubated for an additional 1 h in a blocking buffer (137 mM NaCl, 2.7 mM KCl, 4.3 mM $Na_2HPO_4$, 1.4 mM $KH_2PO_4$, 0.05 % Tween 20, pH 7.4) and were further washed with washing buffer (137 mM NaCl, 2.7 mM KCl, 4.3 mM $Na_2HPO_4$, and 1.4 mM $KH_2PO_4$, 0.01 % Tween 20, pH 7.4). To measure the $K_d$, the prepared kanamycin-magnetic beads (0.2 mg) were incubated with a FAM-labeled aptamer for 1 h at room temperature in 100 μL of binding buffer (20 mM Tris-HCl, 50 mM NaCl, 5 mM KCl, 5 mM $MgCl_2$, pH 8.0) and the unbonded aptamers were removed by washing. The amount of bonded FAM-labeled aptamers on the kanamycin-immobilized magnetic beads was measured by fluorescence (1420 Victor Multilabel Counter, Perkin–Elmer, USA) at 520 nm ($\lambda_{exc}$=494 nm). The measured fluorescence intensities of various concentrations of the FAM-aptamer were analyzed as a saturation curve using the origin program. The $K_d$ was calculated using nonlinear regression analysis.

## 3 Results and Discussion

### 3.1 Aptamers for Kanamycin

The seven selected aptamer sequences (S1–S7) that were obtained through the SELEX procedure and a randomly designed control ssDNA sequence (S8) are listed in Table 1. It is interesting to note that all of the aptamers consist of similar consensus sequences (highlighted regions) which are obviously not present in the control sequence. These conserved regions are present in all of the cloned aptamers (S1–S7) and thus play an important role in the specific binding with kanamycin. To evaluate the binding affinity of the aptamers, all seven aptamers were simultaneously immobilized onto the MAEs chip and were individually evaluated using voltammetry.

### 3.2 Characterization of the MAEs

The modification of the MAEs was characterized by XPS. All XPS spectra were obtained after 10 s of Ar ion gas etching and were calibrated using the C1s peak at 284.6 eV as an internal standard. Figure 2 shows the XPS survey spectra for the unmodified MAEs, the AuNPs/

  

Table 1. Sequence analysis.

| No. | Sequences from 5′ to 3′ |
|---|---|
| S1 | TGGGGGTTGAGGCTAAGCCGAC |
| S2 | TGTCCAAGTGGTCTTGAGGTT |
| S3 | GAAGTAAAGAAGGCTTGAGGGG |
| S4 | GTTGCGTTGGAAGGCACGAATT |
| S5 | TACGTGATTTGGAGGTCGAAGT |
| S6 | GTGTCGACCTGGCGGTTGAACT |
| S7 | GTAGGGTTGGCAGGGGCTTAAGCCTTC |
| S8 | ATGCTACTGCTGCTGCGATCGA |

MAEs, the pTTCA/AuNPs/MAEs, and the aptamer/pTTCA/AuNPs/MAEs. The C1s peak was evident at 284.6 eV due to the C–C and C–H bonds, while the O1s peak was observed at 532.1 eV for all surfaces. Compared with the spectrum for the MAEs, two Au4f peaks were observed at 86.2 eV and 83.6 eV in the spectrum for the AuNPs/MAEs, indicating the successful deposition of AuNPs onto the surface of MAEs. The intensity of Au4f peaks decreased after the formation of the pTTCA film because of the coverage of polymer film on the AuNPs layer, as was reported earlier [27]. A S2p peak that was related to the C–S bond was observed at 163.4 eV in the spectrum for the pTTCA/AuNPs/MAEs. A N1s peak corresponding to the C–N bond was observed at 399.5 eV in the spectrum for the aptamer/pTTCA/AuNPs/MAEs, indicating the successful immobilization of the aptamer. Moreover, a Psp peak appeared at 131.9 eV, which corresponded to phosphate, the major structural component of the aptamer backbone [28]. This finding further demonstrated the successful immobilization of the aptamer.

### 3.3 Electrochemical Behavior of Kanamycin

First, in order to determine the redox peaks position of kanamycin, kanamycin was directly immobilized onto the pTTCA/AuNPs/MAE through the covalent bond formation between the $-NH_2$ groups of kanamycin and the –COOH groups of pTTCA. CV was recorded for the kanamycin-bonded pTTCA by cycling the potential from −0.1 V to 0.5 V in 0.1 M PBS (pH 7.2), as shown in Figure 3. In the CV, a pair of redox peaks of kanamycin was observed at 0.23/0.08 V (dashed line). In contrast, no redox peaks were found in the CV that was recorded for the pTTCA/AuNPs/MAE in the absence of kanamycin (solid line). This indicated that the observed peaks were only due to the electrochemical behavior of kanamycin that was immobilized on the pTTCA/AuNPs/MAE. In the kanamycin structure, the carbohydrate moiety was expected to be electroactive at modest potentials [29,30]. Subsequently, CV was recorded to study the electrochemical behavior of kanamycin that was captured by the aptamer S1-immobilized MAE in 0.1 M PBS (pH 7.2). The CV for the aptamer/pTTCA/AuNPs/MAE did not show any redox peaks (dotted line), whereas a pair of redox peaks was observed at 0.26/0.08 V after incubation in 0.1 M PBS containing 50 μM kanamycin (dashed dotted line). The pair of redox peaks was observed due to the successful capture of kanamycin by the aptamer. Compared to the redox peaks for kanamycin that was directly immobilized on pTTCA, the oxidation peak potential of kanamycin that was captured by aptamer shifted towards the positive direction due to the complex formation between kanamycin and aptamer. On the basis of this finding, it is possible to speculate that the aptamer immobilized on MAE captured kanamycin molecules by forming the a secondary structure. The formation of the kanamycin-aptamer complex caused the electrochemical property of kanamycin to be more stable than that without aptamer binding, and a higher energy was required to oxidize kanamycin that was captured in the complex. Thus, the oxidation potential shifted in the positive direction. In contrast, the reduction peak potential of kanamycin appearing in the reverse scan did not significantly change compared to the reduction peak of kanamycin that was directly attached onto the pTTCA, because of the change of the binding affinity of kanamycin to aptamer after the oxidation. Therefore, the oxidation peak response of kanamycin was used to evaluate the aptamer binding affinity in the subsequent experiments.

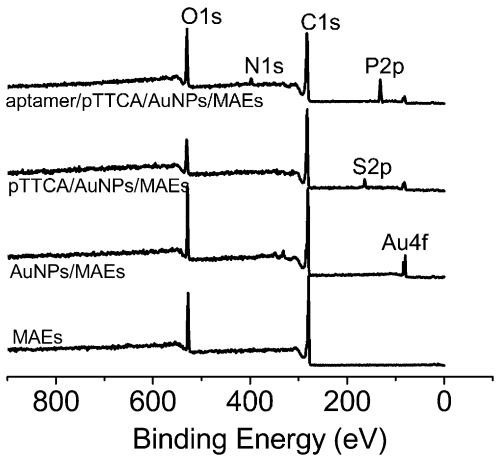


Fig. 2. XPS survey spectra of MAEs, AuNPs/MAEs, pTTCA/AuNPs/MAEs, and aptamer/pTTCA/AuNPs/MAEs.

### 3.4 Qualitative Estimation of Aptamer Binding Affinity

Since the complexation affects the stability of kanamycin involved in the kanamycin-aptamer complex and causes a potential shift of it compared to that of the free form [20], it is possible to screen the aptamer that possesses the highest binding affinity to kanamycin by analyzing the potential shifts. For this purpose, the MAEs chip that was modified with the seven selected aptamers (S1–S7) and a control ssDNA sequence (S8) was used to capture the same concentration of kanamycin (50 μM), followed by washing with PBS. Afterward, LSVs were recorded in 0.1 M PBS for the oxidation of kanamycin captured by all the sequences that were immobilized onto the MAEs, as shown in Figure 4A. All of the LSVs that were recorded

  

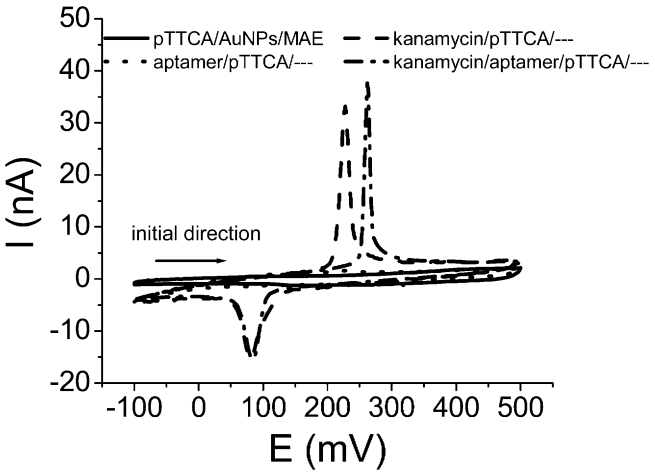


Fig. 3. Cyclic voltammograms of pTTCA/AuNPs/MAE (solid line), kanamycin/pTTCA/AuNPs/MAE (dashed line), aptamer/pTTCA/AuNPs/MAE (dotted line) and kanamycin-aptamer/pTTCA/AuNPs/MAE (dashed dotted line) in 0.1 M PBS (pH 7.2).

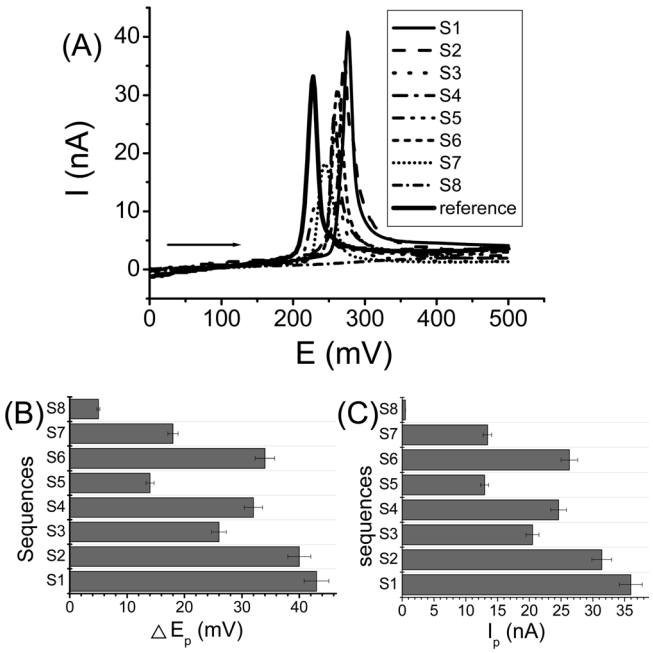


Fig. 4. (A) Linear sweep voltammograms of aptamer (S1–S7)/pTTCA/AuNPs/MAEs after interaction with 50 μM kanamycin recorded in 0.1 M PBS (pH 7.2). (B) Potential shift analysis. (C) Current response analysis.

for the kanamycin-aptamer(S1–S7)/pTTCA/AuNPs/MAEs show the oxidation peak of kanamycin. In contrast, the response of the control sequence S8 was negligible. The different responses of the probes that were modified with the seven aptamers and with the control sequence S8 indicated that kanamycin could only be captured by specific aptamers. Interestingly, the LSVs recorded for kanamycin that was captured by the seven aptamers exhibited different oxidation potentials. To confirm the oxidation potential shift of kanamycin that was involved in the kanamycin-aptamer complexation, the LSV of kanamycin/pTTCA/AuNPs/MAE in a 0.1 M PBS (pH 7.2), which shows an oxidation peak of kanamycin at 0.23 V, was selected as the reference. For each kanamycin-aptamer/pTTCA/AuNPs/MAE, the average value of the potential shift relative to the potential of kanamycin without aptamer binding (0.23 V) was calculated based on five measurements, as shown in Figure 4B. Aptamer S1 showed the maximum potential shift of $43 \pm 1.7$ mV, which was followed closely by S2 ($40 \pm 1.5$ mV). The remaining aptamers and their potential shifts were, in decreasing order: S6 ($34 \pm 1.4$ mV) > S4 ($32 \pm 1.1$ mV) > S3 ($26 \pm 1.0$ mV) > S7 ($18 \pm 0.7$ mV) > S5 ($14 \pm 0.6$ mV). The relative potential shifts were due to the formation of the kanamycin-aptamer complexes, which affected the free energy that was required for the oxidation of kanamycin. Thus, the binding affinity of these aptamers, from highest to lowest, progressed from S1 > S2 > S6 > S4 > S3 > S7 > S5 ⋙ > S8. Furthermore, the data were also analyzed in terms of current response. Interestingly, the oxidation peak currents for kanamycin-aptamer/pTTCA/AuNPs/MAEs modified with different aptamers decreased in the following order: S1 ($35.9 \pm 1.6$ nA) > S2 ($31.4 \pm 1.1$ nA) > S6 ($26.3 \pm 1.0$ nA) > S4 ($24.6 \pm 0.9$ nA) > S3 ($20.5 \pm 0.7$ nA) > S7 ($13.4 \pm 0.6$ nA) > S5 ($12.9 \pm 0.5$ nA) (Figure 4C). These results indicated a decreasing binding affinity to kanamycin in the following order: S1 > S2 > S6 > S4 > S3 > S7 > S5 ⋙ S8, which was the same order from the potential shift analysis. These results corroborated the results that were obtained based on potential shifts. Under the same experimental conditions, the various responses of the seven aptamers were obviously due to the different binding affinity of the aptamers toward kanamycin. The highest response of aptamer S1 indicated that it possessed the highest binding affinity toward kanamycin. The relative standard deviation for the potential shifts and current responses were less than 5% ($n = 5$), indicating a high reproducibility and reliability of the proposed method for evaluating the aptamer binding affinity.

### 3.5 Quantitative Determination of Aptamer Binding Affinity

To further confirm our hypothesis of evaluating aptamer binding affinity using the present method, the $K_d$ between each aptamer and kanamycin was determined based on the current responses of each aptamer to varying concentrations of kanamycin. LSVs recorded for the aptamer S1 probe with varying concentrations of kanamycin are shown as the inset of Figure 5A. Fractional saturation ($F_s$) was determined from the obtained current signal, which is similar to the fluorescence method [31].

$$F_s = \frac{I - I_{min}}{I_{max} - I_{min}} \quad (1)$$

where $I$ is the current signal with varying concentrations of kanamycin, $I_{min}$ is the background current signal, and $I_{max}$ is the maximum current signal at completed saturation. Since the kanamycin concentration was much higher than the amount of aptamer immobilized on MAE, the change of kanamycin concentration before and after the reaction with the immobilized aptamers was negligible. Thus, the free kanamycin concentration after the reaction approximately equaled the kanamycin concentration before the reaction. The fractional saturation, $F_s$ was then plotted against kanamycin concentration ($c_{KAN}$) (Figure 5A), and the saturation isotherm was fitted to the below equation using an origin program [31]

$$F_s = \frac{B_{max} \cdot c_{KAN}}{K_d + c_{KAN}} \quad (2)$$

As a result, the $K_d$ value between aptamer S1 and kanamycin was determined to be $38.06 \pm 0.73$ nM. Similarly, the $K_d$ values between other aptamers (S2–S7) and kanamycin were determined to be $100.09 \pm 4.12$, $978.4 \pm 45.71$, $490.67 \pm 17.47$, $3100.78 \pm 129.44$, $262.99 \pm 10.78$, and $2180.79 \pm 96.43$ nM, respectively. The lowest $K_d$ was obtained between the S1 aptamer and kanamycin, followed by S2, S6, S4, S3, S7, and S5, which showed the decreasing binding affinity toward kanamycin and was in accord with the above qualitative results. The lowest $K_d$ that was obtained between aptamer S1 and kanamycin indicated that, among the seven selected aptamers, S1 bound kanamycin with the highest binding affinity. To confirm the obtained results, a conventional method using FAM-labeled fluorescence measurements to determine $K_d$ values was performed on four randomly selected aptamers. The $K_d$ values for S1, S2, S4, and S7 were determined by the fluorescence method to be $78.8 \pm 3.5$, $182 \pm 8.2$, $640 \pm 29.9$, and $2590 \pm 106.7$ nM, respectively (Figure 5B), indicating the decreasing binding affinity in the following order: S1 > S2 > S4 > S7. Compared to the fluorescence method, the results based on the current responses exhibited the same patterns in binding affinity, which supported our hypothesis for being able to evaluate the binding affinity of the aptamers using the present method. Furthermore, the ability to evaluate aptamer affinity using the present method demonstrates marked advantages over the fluorescence method because it is simple, fast, inexpensive, and label-free. The ability of the MAEs chip to provide both qualitative and quantitative results further establishes the present method as a powerful tool that can simultaneously analyze the binding affinity of a series of aptamers that are obtained from cloning. To investigate the specificity of the selected aptamers toward kanamycin, a negative control experiment using ampicillin was performed under the same conditions. As a result, no response was observed, indicating the good specificity of the selected aptamers toward kanamycin.

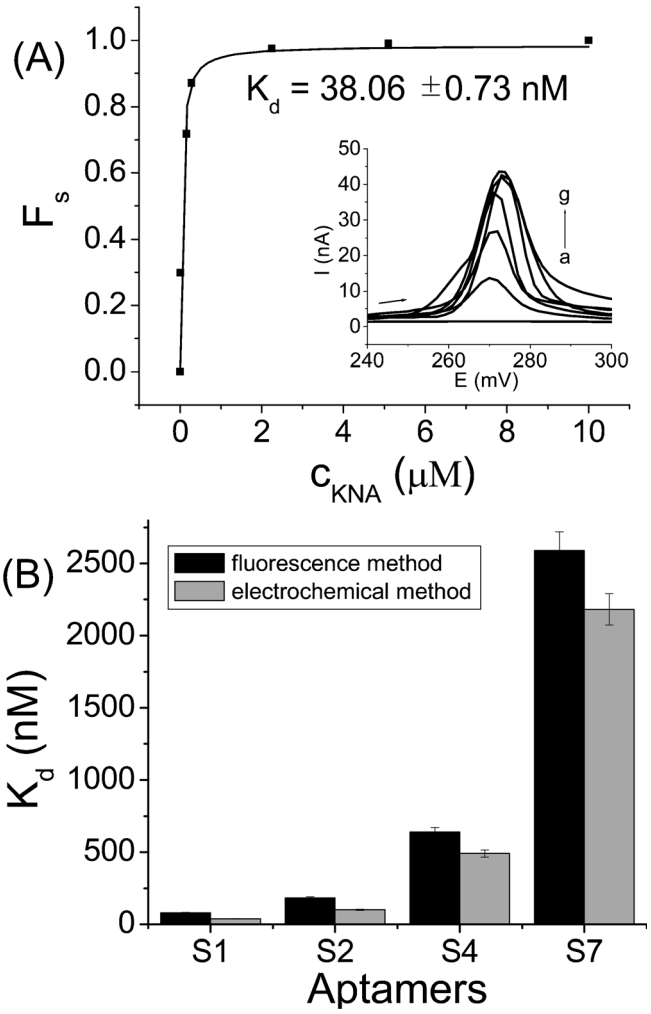


Fig. 5. (A) The fractional saturation of the aptamer S1 plotted against the concentration of free kanamycin and fitted to a single binding site model. Inset: Current responses of aptamer S1/pTTCA/AuNPs/MAEs to varying concentrations of kanamycin: (a) 0, (b) 0.05, (c) 0.1, (d) 0.5, (e) 2.5, (f) 5.0, and (g) 10.0 μM. (B) Comparison of the $K_d$ values obtained using fluorescence method (black) and electrocehmical method (gray).

### 3.6 Secondary Structure Analysis of Aptamers

To further investigate the binding affinity of the seven aptamers toward kanamycin, the secondary structures of these aptamers (S1–S7) were predicted using a web-based *m*-fold software [21] (Figure 6) and were discussed based on the electrochemical responses. These structures exhibited typical stem and loop motifs. High electrochemical responses were obtained for S1, S2, and S6, which possessed somewhat similar secondary structures. The GG in the aptamer sequence was in the center position of the loop and equal numbers of GC and TA bonds were observed in the stem region, which resulted in quite similar secondary structures for S1 and S2 in the. The conserved sequence motif of TTGAGG was located at the juncture of the stem and loop structure in S1, and a similar sequence was positioned at the stem in S2 and S6. Since the highest response was obtained for aptamer S1, the loca-

  

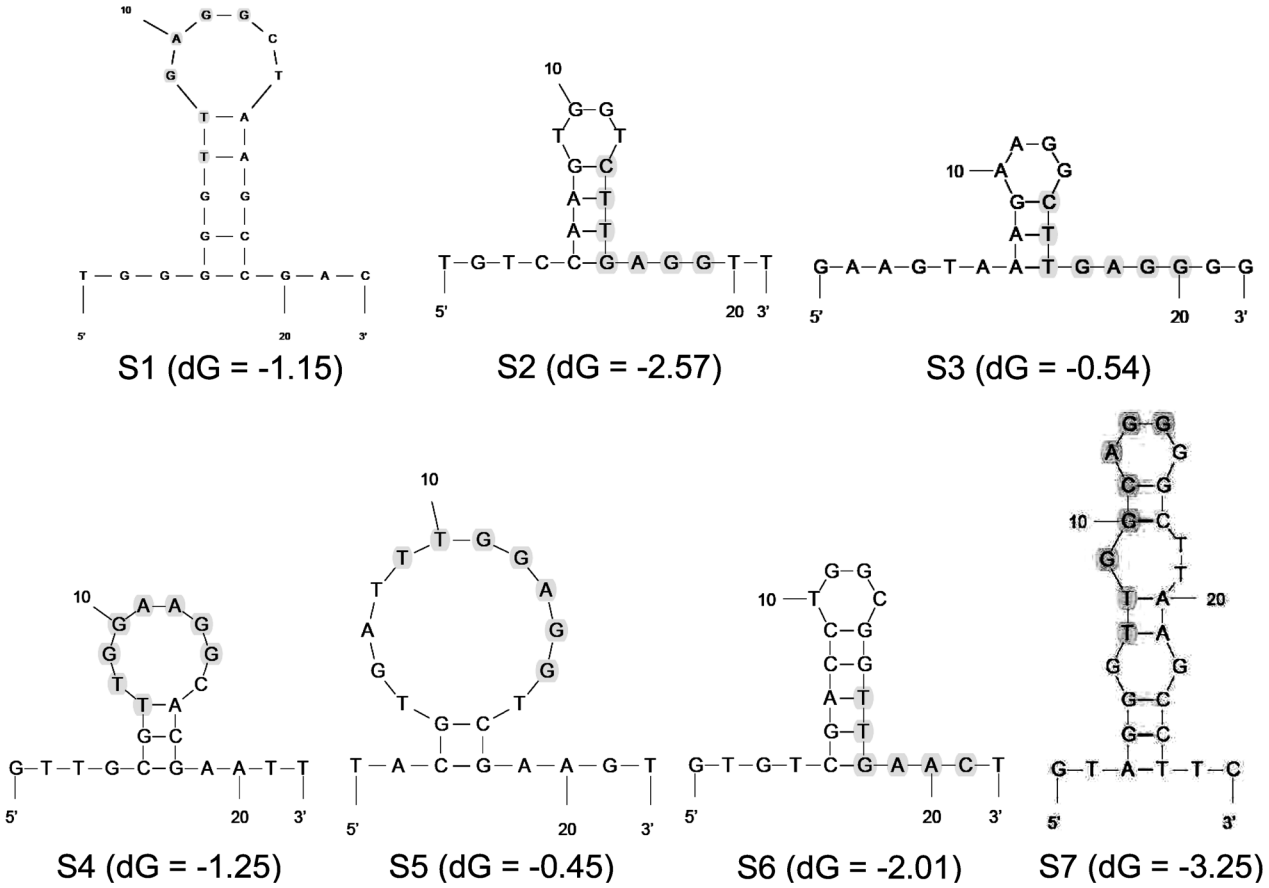


Fig. 6. Secondary structures of selected aptamers as predicted by *m*-fold. dG is Gibbs energy (kcal/mol).

tion of the consensus sequence at the juncture of the stem and loop structure might show higher affinity to kanamycin than the position in the stem. There was also a GG center in the loop of S7, and the TTGGC consensus sequence was located in the stem. Its secondary structure, however, was too complicated, and the considerable distance between the GG center and the TA bond might have made it difficult to bind to kanamycin. Thus, a low electrochemical response was obtained for S7. Compared to S1, S2, and S6, lower responses were obtained for S3 and S4. Both of these aptamers contained GG in the loop region but not in the center position. A consensus sequence TTGAGG was observed in the stem of S3, while a consensus sequence TTGGAAGG was found at the loop and stem juncture of S4. In addition, the stability of secondary structure of S3 ($dG = -0.54$) is lower than that of S4 ($dG = -1.25$). Both the location of consensus sequence and the stability based on Gibbs free energy might be responsible for lower response of S3 than that of S4. In the secondary structure of S5, a consensus sequence TTGGAGG was located in the loop. The GG, however, was not in the center of the loop, and there was no AT bond in the stem. Additionally, the stability of that structure is very low ($dG = -0.45$). Thus, the lowest response was obtained in this case.

Therefore, we believe that the consensus sequence TTGAGG or similar sequences there are derived from TTGAGG play an important role in capturing kanamycin by different aptamers. The GG in the loop and the AT bond in the stem of the secondary structure of aptamer also appears to affect the capture of kanamycin. The secondary structure analysis was consistent with the electrochemical analysis results, which supported our hypothesis of being able to evaluate the binding affinity of aptamers toward kanamycin using the present method.

## 4 Conclusions

An electrochemical method using the microarray chip was successfully developed to evaluate the binding affinity of a series of aptamers. Kanamycin was used as a model compound and the aptamer having the highest binding affinity was selected by exploring the potential shifts and the current responses revealed by the aptamer-kanamycin interaction. The results show the same trend to that determined using a conventional fluorescence method, which is validating the present method for binding affinity evaluation. We successfully selected the aptamer having the highest binding affinity. The present method offers many advantages over conventional fluo-

  

rescence method, enabling a label-free, simple, high throughput, and low-cost method for evaluating aptamer binding affinity. It will be a potential tool for aptamer selection and can be used to elucidate the binding affinity of diverse aptamer library. This simple method will be very helpful in the search of the most selective aptamers toward target which can be used for various analysis purposes.

## Acknowledgements

This work was supported by the National Research Fund Grant funded by the *Ministry of Education, Science and Technology,* South Korea (Grant No. 20100029128).

## References

[1] D. S. Wilson, J. W. Szostak, *Annu. Rev. Biochem.* **1999**, *68*, 611.
[2] T. Herman, D. Patel, *Science* **2000**, *287*, 820.
[3] S. D. Jayasena, *Clin. Chem.* **1999**, *45*, 1628.
[4] A. D. Ellington, J. W. Szostak, *Nature* **1990**, *346*, 818.
[5] C. Tuerk, L. Gold, *Science* **1990**, *249*, 505.
[6] K. Gebhardt, A. Shokraei, E. Babaie, B. H. Lindqvist, *Biochemistry* **2000**, *39*, 7255.
[7] J. H. Davis, J. W. Szostak, *Proc. Natl. Acad. Sci. USA* **2002**, *99*, 11616.
[8] Y. S. Kim, C. J. Hyun, I. A. Kim, M. B. Gu, *Bioorg. Med. Chem.* **2010**, *18*, 3467.
[9] H. Schürer, A. Buchynskyy, K. Korn, M. Famulok, P. Welzel, U. Hahn, *Biol. Chem.* **2001**, *382*, 479.
[10] Z. Tang, D. Shangguan, K. Wang, H. Shi, K. Sefah, P. Mallikratchy, H. W. Chen, Y. Li, W. Tan, *Anal. Chem.* **2007**, *79*, 4900.
[11] M. Cho, Y. Xiao, J. Nie, R. Stewart, A. T. Csordas, S. S. Oh, J. A. Thomson, H. T. Soh, *Proc. Natl. Acad. Sci. USA* **2010**, *107*, 15373.
[12] M. Hendrix, E. S. Priestley, G. F. Joyce, C. H. Wong, *J. Am. Chem. Soc.* **1997**, *119*, 3641.
[13] S. H. L. Verhelst, P. J. A. Michiels, G. A. Marel, C. A. A. Boeckel, J. H. Boom, *ChemBioChem* **2004**, *5*, 937.
[14] M. N. Win, J. S. Klein, C. D. Smolke, *Nucleic Acids Res.* **2006**, *34*, 5670.
[15] A. Drabovich, M. Berezovski, S. N. Krylov, *J. Am. Chem. Soc.* **2005**, *127*, 11224.
[16] A. P. Drabovich, M. Berezovski, V. Okhonin, S. N. Krylov, *Anal. Chem.* **2006**, *78*, 3171.
[17] Y. Miyachi, N. Shimizu, C. Oginol, A. Kondo, *Nucleic Acids Res.* **2010**, *38*, e21.
[18] T. Hianik, J. Wang, *Electroanalysis* **2009**, *21*, 1223.
[19] J. Wang, *Analytical Electrochemistry*, Wiley, New York **2000**.
[20] A. J. Bard, L. R. Faulkner, *Electrochemical Methods*, 2nd ed., Wiley, New York **2001**, pp. 186–190, 594–595.
[21] M. Zuker, *Nucleic Acids Res.* **2003**, *31*, 3406.
[22] K.-M. Song, M. Cho, H. Jo, K. Min, S. H. Jeon, T. Kim, M. S. Han, J. K. Ku, C. Ban, *Anal. Biochem.* **2011**, *415*, 175.
[23] T.-Y. Lee, Y.-B. Shim, *Anal. Chem.* **2001**, *73*, 5629.
[24] M. J. A. Shiddiky, Y.-B. Shim, *Anal. Chem.* **2007**, *79*, 3724.
[25] K.-S. Lee, M.-S. Won, H.-B. Noh, Y.-B. Shim, *Biomaterials* **2010**, *31*, 7827.
[26] F. Darain, S.-U. Park, Y.-B. Shim, *Biosens. Bioelectron.* **2003**, *18*, 773.
[27] Y. Zhu, J. I. Son, Y.-B. Shim, *Biosens. Bioelectron.* **2010**, *26*, 1002.
[28] P. Chandra, H.-B. Noh, M.-S. Won, Y.-B. Shim, *Biosens. Bioelectron.* **2011**, *26*, 4442.
[29] P. D. Vnegel, R. P. Baldwin, *Electroanalysis* **1997**, *9*, 1145.
[30] X. Lu, M. Zhang, J. Kang, X. Wang, L. Zhuo, H. Liu, *J. Inorg. Biochem.* **2004**, *98*, 582.
[31] M. Muller, J. E. Weigand, O. Weichenrieder, B. Suess, *Nucleic Acids Res.* **2006**, *34*, 2607.

  